

Edit3K: Universal Representation Learning for Video Editing Components

Xin Gu^{1,2,†,‡}, Libo Zhang^{2,3,†}, Fan Chen¹, Longyin Wen¹, Yufei Wang¹, Tiejian Luo², Sijie Zhu^{1,*}

¹ByteDance Inc. ²University of Chinese Academy of Sciences

³Institute of Software Chinese Academy of Sciences

{fan.chen, longyin.wen, yufei.wang, sijiezhu}@bytedance.com

guxin21@mails.ucas.edu.cn, libo@iscas.ac.cn, tjluo@ucas.ac.cn

Abstract

This paper focuses on understanding the predominant video creation pipeline, i.e., compositional video editing with six main types of editing components, including video effects, animation, transition, filter, sticker, and text. In contrast to existing visual representation learning of visual materials (i.e., images/videos), we aim to learn visual representations of editing actions/components that are generally applied on raw materials. We start by proposing the first large-scale dataset for editing components of video creation, which covers about 3,094 editing components with 618,800 videos. Each video in our dataset is rendered by various image/video materials with a single editing component, which supports atomic visual understanding of different editing components. It can also benefit several downstream tasks, e.g., editing component recommendation, editing component recognition/retrieval, etc. Existing visual representation methods perform poorly because it is difficult to disentangle the visual appearance of editing components from raw materials. To that end, we benchmark popular alternative solutions and propose a novel method that learns to attend to the appearance of editing components regardless of raw materials. Our method achieves favorable results on editing component retrieval/recognition compared to the alternative solutions. A user study is also conducted to show that our representations cluster visually similar editing components better than other alternatives. Furthermore, our learned representations used to transition recommendation tasks achieve state-of-the-art results on the AutoTransition dataset. The code and dataset will be released for academic use.

* Corresponding author, sijiezhu@bytedance.com

† Equal contribution

‡ This work was done during the first author's internship at ByteDance

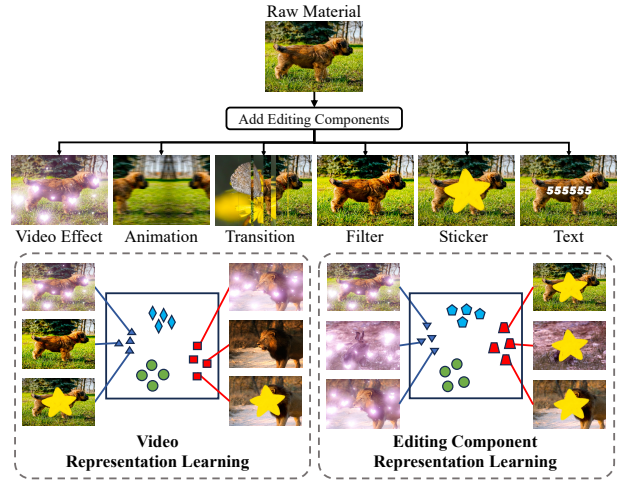


Figure 1. An overview of generic video representation learning and editing components representation learning. The embedding of generic video representation learning is clustered based on video content, e.g., semantics, context, etc, while the ideal editing component representation should be only dependent on the applied editing components rather than the content of raw materials.

1. Introduction

Video has emerged as a major modality of data across various applications, including social media, advertising, education, and entertainment. The predominant video creation pipeline for production, i.e., compositional video editing, is based on the combination of editing components (Fig. 1), e.g., video effect, animation, transition, filter, sticker, and text. Tons of videos are created with these editing components every day on various video creation platforms, but little effort has been made to understand these editing components. Specifically, learning universal representations for editing components is unexplored but critical for lots of downstream tasks in video creation fields, e.g., effects recommendation, detection, recognition, generation, etc.

Existing video representation learning methods [9, 14,

[28, 32, 33] are usually developed on object-centric action recognition datasets, *e.g.*, Kinetics [16], to encode the information from the video content, *e.g.*, semantics, the action of the subjective, context, motion, etc. However, editing components usually do not have clear semantics, subjective action, or context information. They could be a simple chroma change of the whole image or local effects like scattering stars. Some components are special homography transformations on the raw material (*i.e.*, image/video) and the rendered result is highly dependent on the appearance of the raw material. Thus, it is extremely challenging to learn a representation that encodes the information of editing components regardless of raw materials. Fig. 1 shows a comparison between generic video representation learning and our task. To the best of our knowledge, how to learn universal representations for diverse types of editing components remains unexplored in representation learning literature, and none of the existing datasets supports research on learning universal representation for the 6 major types of video editing components.

In this paper, we propose the first large-scale video editing components dataset, *i.e.*, Edit3K, to facilitate research on editing components and automatic video editing. The proposed dataset contains 618,800 videos covering 3,094 editing components of 6 major types. Each video is rendered with one editing component with both image and video materials to enable atomic research on single editing components. Given that the editing component is visually mixed with raw materials, the key challenge of this problem is to distinguish editing components in the rendered frames but ignore the changes in the raw materials. We benchmark popular representation learning methods, *e.g.*, contrastive learning and masked autoencoder, and propose a tailored contrastive learning loss that better solves this problem. In addition, we propose a novel embedding guidance architecture that enhances the distinguishing ability of editing components by providing feedback from the output embedding to the model. The learned editing element representations of our method can be directly applied to downstream tasks *e.g.*, transition recommendation [27], achieving state-of-the-art results. Attention map visualization shows that our model learns to focus on the editing components without pixel-level supervision. We summarize our contributions as follows:

- We introduce the first large-scale dataset for video editing components covering 3,094 atomic editing actions of 6 major categories, which makes it possible to learn universal representations for all 6 categories of editing components.
- We propose a novel embedding guidance architecture that aims to distinguish the editing components and raw materials, along with a specifically designed contrastive learning loss to guide the training process.

- We benchmark major alternative methods and validate the superiority of our method in various scenarios. Extensive experiments show state-of-art performance on both Edit3K and AutoTransition datasets.

2. Related Work

Video Editing/Creation Conventional workflow of video editing requires a deep understanding of the raw image/video materials and professional knowledge of editing and aesthetics, *e.g.*, manually cutting videos and selecting editing effects, thus is extremely time-consuming for the video creators. Automatic video editing can significantly improve editing efficiency and it has been explored from different perspectives [11, 18, 27]. Koorathota *et al.* [18] focus on contextual and multimodal understanding for video editing. Frey *et al.* [11] transfer editing styles from a source video to a target video with matched footage, considering framing, content type, playback speed, and lighting of input video segments. AutoTransition [27] proposes to automatically recommend transitions based on the previous video frames and audio. Recently, there has been a thread of works [4, 19, 35] using GAN [12] or diffusion [15, 25] model to generate videos, but they are still not widely deployed in real-world video creation applications. *We consider them as orthogonal works and they could be combined with our work in the future.*

Editing Components for Video Creation To the best of our knowledge, none of the existing works provides a comprehensive study on video editing components. The most related work, AutoTransition [27] is proposed for a specific downstream task, *i.e.*, transition recommendation. The AutoTransition dataset contains 104 transitions and only 30 transitions are used for the transition recommendation task. *This work only focuses on one specific type and does not support learning universal representation for all the major 6 types of editing components.*

Visual Representation Learning Visual representation learning has been extensively studied for video data [10]. Early works conduct supervised classification [9, 29] on large-scale datasets, *e.g.*, Kinetics [16], to learn strong pre-trained representation. Recent self-supervised representation learning methods, *e.g.*, contrastive learning [5, 13, 21, 22] and masked autoencoder [2, 14, 28], have achieved comparable performance as supervised methods on downstream tasks [10]. The key insight is to learn a representation space where visually similar videos are close to each other. *However, existing works have limitations on learning representation for editing components from video data (Sec. 5.2), because these methods are not designed to distinguish the raw material and editing components in the video frames.*

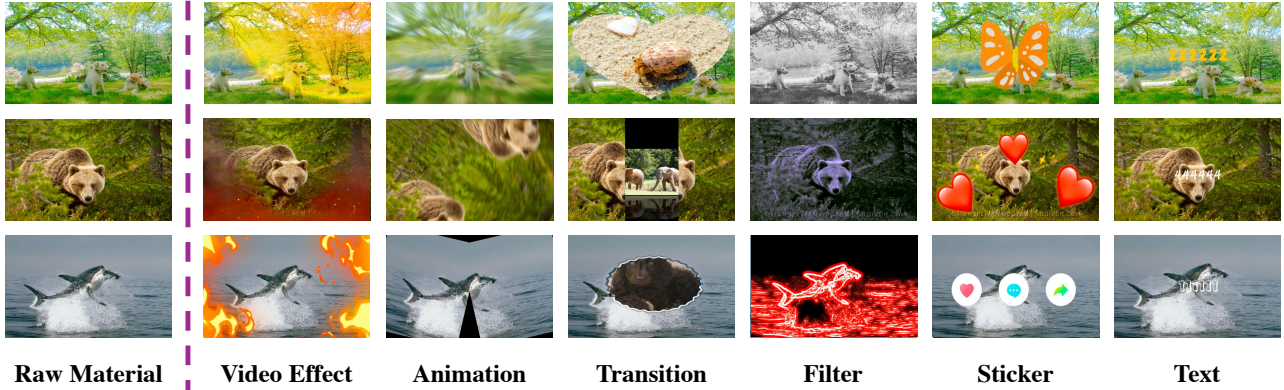


Figure 2. Examples of 6 major types of video editing components, *i.e.*, video effect, animation, transition, filter, sticker, and text.

| | Video Effect | Animation | Transition | Filter | Sticker | Text | Total |
|-----------------|--------------|-----------|------------|--------|---------|---------|----------------|
| Classes | 888 | 176 | 204 | 228 | 1000 | 598 | 3,094 |
| Rendered Videos | 177,600 | 35,200 | 40,800 | 45,600 | 200,000 | 119,600 | 618,800 |

Table 1. The statistical information of the proposed Edit3K dataset.

3. Edit3K Dataset

Existing video datasets mostly focus on understanding the overall content of the video frames, *e.g.*, action, context, semantics, and geometry, which can not support the research for understanding video editing components. The most related dataset is proposed in AutoTransition [27], but this dataset only contains one editing component type (*i.e.*, 104 transitions) out of the major six types with limited coverage. To the best of our knowledge, our dataset is the first large-scale editing component dataset for video creation covering all the six major types, *i.e.*, video effect, animation, transition, filter, sticker, and text.

3.1. Editing Component Definition

There is no formal definition for the 6 types of editing components in the academic literature, so we summarize the major difference between them and describe their connection with existing concepts. Examples are shown in Fig. 2.

Both video effects and filters change the appearance of material images or video frames toward a specific style, but video effects focus more on local editing, *e.g.*, adding shining star-shaped markers. Filters mainly change the overall style of the whole scene, *e.g.*, adjusting the illumination and chroma. Animation can be considered as a homography transformation applied to the whole material, which is similar to camera viewpoint changes. The transition is applied to connect two materials with appearance changes and fast motion. The sticker simply uses copy-paste to add another foreground object on top of the current material, which is similar to image composition [36]. However, some of the

stickers are video stickers and the stickers may look different in each frame. Text is a special sticker whose content can be edited by the user, but the text style can be changed by applying different fonts. We focus on text font/style rather than the content in this paper.

3.2. Dataset Generation

It is challenging to collect an academic dataset for editing components because online published videos [27] usually apply multiple editing components sparsely in an entangled way. Most of the frames may contain no editing component or only a simple filter, while a small number of frames (*e.g.* a 0.5 s slot) could have stickers/text, video effects, and animations at the same time. To address this limitation, we propose to render videos based on existing raw materials and a pre-defined set of editing components using a free-to-use video editing tool, *i.e.*, *CapCut* [1]. Each video only contains one disentangled editing component to support atomic research on all editing components with a balanced distribution.

We use images and videos from the ImageNet [6] and ImageNet-Vid [6, 26] datasets as raw materials for rendering. For each video, we randomly take two images/videos as the source material pair for two video slots, and each slot lasts 2 seconds. If the component is a transition, we add it between the two slots, which lasts for 2s, and each slot is reduced to 1s. Otherwise, we apply the component on both the two slots, which covers 4s. In total, we generate 618,800 videos covering 3,094 editing components.

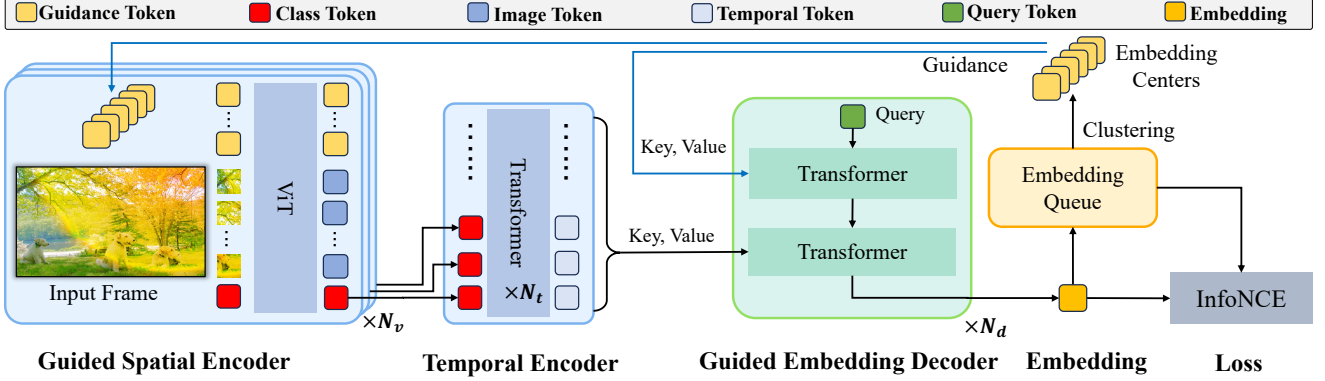


Figure 3. An overview of the proposed method. The input video frames are fed to the spatial and temporal encoder to generate the visual features. Then the embedding decoder takes the visual features as key, value and generates the final editing component embeddings using cross-attention mechanism with one query token. All encoders and decoders are guided with guidance tokens which are the embedding centers of the embedding saved in a queue. The model is optimized with InfoNCE [13, 21] loss across the batch and the embedding queue provides extra negative samples for an extra loss term. Best viewed on screen with zoom-in.

3.3. Dataset Statistics

Tab. 1 shows the detailed statistical information of the 6 categories of editing components in the proposed dataset. Our dataset contains significantly ($29.75\times$) more editing components than AutoTransition [27] dataset. Unlike AutoTransition [27] which adopts online published videos with unbalanced distribution, our dataset is more balanced across different editing components which is critical for representation learning. Our dataset is the first one to provide editing components with static image materials, which provides valuable research source data for understanding the motion effect of editing components.

4. Method

Fig. 3 shows an overview of the proposed method. We first formulate the problem in Sec. 4.1. Then we describe the guided spatial-temporal encoder in Sec. 4.2 and the guided embedding decoder in Sec. 4.3. Sec. 4.4 introduces the embedding queue mechanism and Sec. 4.5 describes the loss function.

4.1. Problem Formulation

Given the input video frames $\mathcal{F} = \{f_i\}_{i=1}^{N_v}$ where $f_i \in \mathbb{R}^{H \times W \times C}$ (H, W, C denote the height, width and channels), the goal of our model is to generate an embedding that encodes the information of the editing component in the video for recognition, recommendation, etc. An ideal embedding should be dependent on the applied editing components but independent of the raw video materials. In addition, we expect visually similar editing components to be close to each other in the embedding space, *e.g.*, all heart-shaped video effects may be distributed in a cluster.

To achieve this goal, we formulate this special representation learning task as a contrastive learning problem.

Given a set of raw material videos $\mathcal{M} = \{m_i\}_{i=1}^{N_m}$ and editing components $\mathcal{E} = \{e_j\}_{j=1}^{N_e}$, we can render each raw video with all the N_e editing components, resulting in $N_m \times N_e$ rendered videos $\{(m_i, e_j)\}$. For the editing component e_k , all the rendered videos using this editing component $\{(m_i, e_k)\}$ are considered as positive samples for each other. On the other hand, all the rendered videos with other editing components $\{(m_i, e_j) | j \neq k\}$ are considered negative samples for e_k . A contrastive loss [13, 21] (Sec. 4.5) is then applied to pull the positive samples closer while pushing the negative samples away in the embedding space.

4.2. Guided Spatial-Temporal Encoder

Guided Spatial Encoder. As shown in Fig. 3, the N_v inputs frames are fed to the spatial encoder separately. We follow ViT [8] to evenly divide the input frame into small patches with the size of 32×32 . The patches are fed to a linear projection layer [8] to generate patch embedding, and positional embedding [8] is added to each embedding to generate the image tokens (blue squares in Fig. 3). To help the model distinguish editing components and raw materials in the rendered frames, we add another set of guidance tokens (yellow squares in Fig. 3) in the input, which will be described in Sec. 4.4. *The guidance tokens can be considered as feedback from the learned embedding to the input and provide the spatial encode with prior knowledge of possible editing components.* The class token (red square in Fig. 3) is concatenated to the input tokens to aggregate the information from all the tokens. The tokens are fed to multiple transformer layers with multi-head self-attention [31], and the output class token of the last transformer layer is used as the output of the whole frame.

Temporal Encoder. For N_v input frames, N_v output

class tokens are generated separately without temporal correlation. However, some editing components, *e.g.*, animation, and transition, contain strong motion information which requires strong temporal information to understand. Therefore, we add a temporal encoder containing N_t self-attention [31] transformer blocks to learn the temporal correlation between frames. In addition, some editing components may be indistinguishable if the sequential information is missing. For example, “move to left transition” played in reverse order is the same as “move to right transition”, so we add position embedding [31] to the input tokens of the temporal encoder to provide sequential information.

4.3. Guided Embedding Decoder

The output tokens of the spatial-temporal encoder contain the mixed information from the editing components and the raw materials. Inspired by end-to-end object detection DETR [3], we leverage the cross-attention [31] mechanism to extract information corresponding to the editing components from the input tokens. As shown in Fig. 3, we first adopt the guidance tokens (Sec. 4.4) as the (key, value) tokens of the cross-attention transformer block [31], which represent the historical embedding of editing components. One query token is fed to the first transformer block to extract prior knowledge of the editing components embedding. The output token is then fed to the second transformer block as the query token and the output of the spatial-temporal encoder is used as (key, value) tokens. The guided embedding decoder contains N_d layers of these two transformer blocks, and the output token of the last layer is used as the final embedding of the input video.

4.4. Embedding Queues

The limited batch size is not able to provide enough hard negative samples for contrastive learning and this issue is typically addressed with sample mining [34] or memory bank/queue [13]. Different from the memory bank in MoCo [13], we build the dynamic embedding queues to save the recently generated embedding corresponding to all editing components instead of the whole video set. For each specific editing component in the training set, we maintain a first-in-first-out (FIFO) queue with the size of 5 to save the most recently generated embedding corresponding to this editing component during training. The memory cost of the embedding queues is negligible, but it provides a large number of negative samples for contrastive learning (Eq. 2). All the embeddings are l_2 -normalized before joining the queue.

Moreover, the embedding queues provide prior knowledge of all the editing components that can be used as guidance to improve the spatial-temporal encoder and the embedding decoder for distinguishing editing components from raw videos. However, using thousands of embedding as guidance tokens would cost a lot in terms of GPU mem-

ory and computation, we thus adopt the embedding centers as the guidance tokens. Since the 6 types of editing components are naturally clustered into 6 corresponding centers in the embedding space, we compute the embedding centers for the 6 types as guidance tokens by default, which involves negligible memory and computation costs. Alternatively, k-means clustering centers also perform well as guidance tokens (Sec. 5.4).

4.5. Loss Function

Our model is optimized with two loss terms, *i.e.*, in-batch loss and embedding queue loss. We adopt the widely used InfoNCE loss [13, 21] formulation but use our task-specific positive and negative definition (Sec. 4.1). We first sample N_b editing components in a batch, *i.e.*, $\{e_i\}_{i=1}^{N_b}$. For each editing component e_i , we randomly select two positive samples, and their embeddings are denoted as q_i and k_i . Apparently, other embeddings in this batch, *e.g.*, $\{k_j\}_{j \neq i}$ are negative samples for q_i because they correspond to different editing components. The in-batch loss is written as:

$$\mathcal{L}_{batch} = \frac{1}{N_b} \sum_{i=1}^{N_b} -\log \frac{\exp(q_i \cdot k_i / \tau)}{\sum_{j=1}^{N_b} \exp(q_i \cdot k_j / \tau)}, \quad (1)$$

where \cdot means the cosine similarity operation between two embeddings and τ is the temperature. Assume that we have N_e editing components in total for the training. There are N_e embedding queues (Sec. 4.4) saving the most recent embeddings generated during training, we take the l_2 -normalized average embedding in each queue as the reference embedding, *i.e.*, $\{r_j\}_{j=1}^{N_e}$. The embedding queue loss term is given as:

$$\mathcal{L}_{queue} = \frac{1}{N_e} \sum_{i=1}^{N_e} -\log \frac{\exp(q_i \cdot r_i / \tau)}{\sum_{j=1}^{N_e} \exp(q_i \cdot r_j / \tau)}. \quad (2)$$

This term covers other hard negative editing components for q_i and improves both the performance and training stability. The final loss is computed as $\mathcal{L} = \mathcal{L}_{batch} + \mathcal{L}_{queue}$.

5. Experiment

5.1. Implementation Details

We implement our method using PyTorch [23]. We use CLIP-B/32 [24] pre-trained weights to initialize the spatial encoder and the remaining modules are all randomly initialized. We follow BERT [7] to implement the self-attention and cross-attention transformer block. For input videos, we uniformly sample $N_v = 16$ frames from each video, and the height H and width W of each frame is resized to 224×224 . We train our model with Adam [17] optimizer and cosine [20] learning rate scheduling. The batch size N_b per GPU is set to 8 by default and all models are trained for 20 epochs.

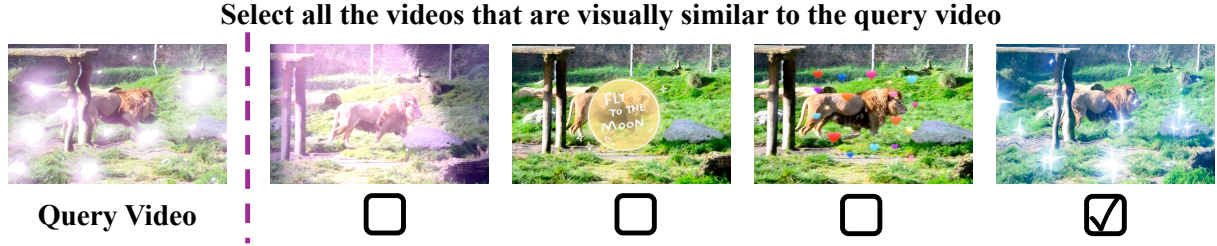


Figure 5. An example from the user study. The users are asked to select all the videos that are visually similar to the query video. Best viewed on screen with zoom-in.

| Method | V. E. | Anim. | Tran. | Filt. | Stic. | Text | Avg. |
|-----------------|-------------|-------------|-------------|-------------|-------------|-------------|-------------|
| Random | 0.9 | 0.9 | 1.6 | 0.9 | 0.8 | 1.3 | 1.1 |
| VideoMoCo | 45.7 | 49.1 | 69.5 | 37.5 | 40.1 | 52.3 | 49.0 |
| Ours (Baseline) | 37.4 | 59.4 | 67.9 | 39.7 | 37.6 | 43.2 | 47.5 |
| Ours | 61.3 | 67.9 | 67.1 | 46.6 | 62.4 | 63.9 | 61.5 |

Table 3. The satisfactory rate (%) of different methods in user study. V.E., Anim., Tran., Filt., Stic. denote video effect, animation, transition, filter, and sticker.

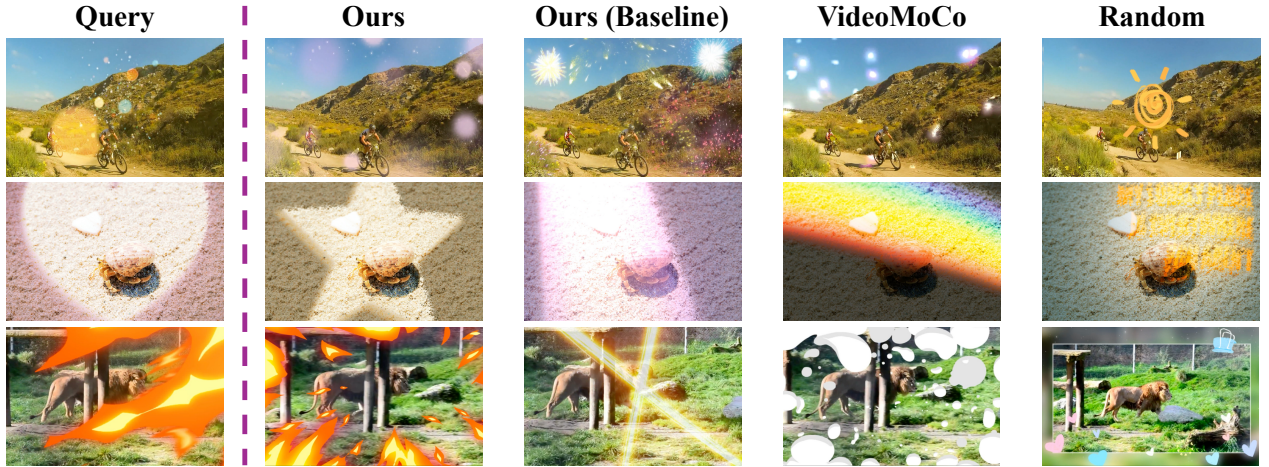


Figure 6. The top-1 similar editing components corresponding to the query editing component using different methods. The similarity is computed based on the embedding centers of editing components and we show one frame of a randomly selected video corresponding to each editing component for visualization. Best viewed with zoom-in.

The users are given 5 videos in a row, where the left column is the video for the query editing component, and the other columns show the example videos for the retrieved editing components corresponding to the 4 methods (an example is shown in Fig. 5). The users are asked to select the videos that are visually similar to the query and each query is evaluated by at least 10 users. The selected results are considered satisfactory and we compute the satisfactory rate of different methods on all queries. As shown in Tab. 3, ‘Ours’ significantly outperforms the other three methods in terms of average satisfactory rate, indicating the effective-

ness of the proposed guidance architecture and additional loss on embedding distribution. The result is also consistent across different editing component categories. Qualitative results is provided in Fig. 6. The t-SNE [30] visualization for the embedding space is provided in the **supplementary material**.

5.4. Ablation Study

Different Modules. We conduct ablation study in Tab. 4 by removing different modules to demonstrate the effectiveness of each module. The ‘Baseline’ model with

| | Video Effect | | Animation | | Transition | | Filter | | Sticker | | Texts | | Avg. | |
|--------------------------------------|--------------|-------------|-------------|-------------|-------------|-------------|-------------|-------------|-------------|-------------|-------------|-------------|-------------|-------------|
| | R@1 | R@10 | R@1 | R@10 | R@1 | R@10 | R@1 | R@10 | R@1 | R@10 | R@1 | R@10 | R@1 | R@10 |
| Baseline | 33.5 | 71.5 | 22.4 | 68.4 | 30.0 | 76.2 | 15.6 | 40.6 | 56.6 | 93.9 | 28.8 | 85.4 | 31.2 | 72.7 |
| Baseline + \mathcal{L}_q | 40.3 | 76.4 | 32.7 | 69.2 | 30.9 | 72.9 | 20.8 | 39.8 | 58.8 | 94.6 | 36.1 | 90.2 | 36.6 | 73.8 |
| Baseline + \mathcal{L}_q + GT | 43.2 | 75.9 | 37.4 | 70.9 | 39.2 | 76.4 | 20.8 | 44.3 | 58.1 | 95.1 | 41.5 | 92.4 | 40.0 | 75.8 |
| Baseline + \mathcal{L}_q + GD | 51.0 | 78.6 | 41.0 | 82.0 | 49.8 | 87.5 | 21.0 | 44.9 | 79.2 | 97.7 | 52.1 | 90.3 | 49.0 | 80.2 |
| Baseline + \mathcal{L}_q + GT + GD | 55.3 | 80.6 | 51.6 | 81.8 | 54.6 | 85.3 | 22.5 | 48.0 | 85.8 | 98.2 | 46.0 | 89.7 | 52.6 | 80.6 |

Table 4. Ablations study for different modules of our method on Edit3K for editing components retrieval in terms of R@k (%). \mathcal{L}_q is the embedding queue loss. ‘GT’ and ‘GD’ represent the guided tokens and guided decoder.

| Method | R@1 | R@10 |
|-----------------|-------------|-------------|
| None | 36.6 | 73.8 |
| K-Means | 52.1 | 79.9 |
| Default 6 Types | 52.6 | 80.6 |

Table 5. Ablation of different methods for generating embedding centers on Edit3K for editing components retrieval in terms of R@k (%).

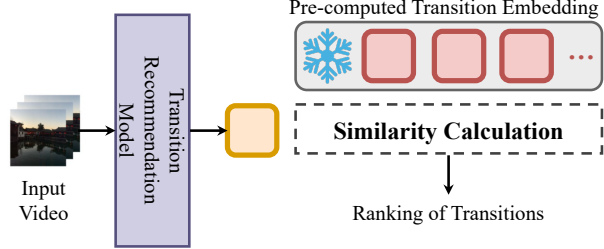


Figure 7. An overview of the transition recommendation pipeline.

| Transition Embedding | | Performance | | |
|----------------------|----------------|--------------|--------------|-----------------------|
| Method | Dataset | R@1 | R@5 | Rank (\downarrow) |
| Random [27] | - | 25.67 | 66.30 | 5.65 |
| Classification[27] | AutoTransition | 28.06 | 66.85 | 5.48 |
| Ours-A | AutoTransition | 28.89 | 67.12 | 4.86 |
| Ours-E | Edit3K | 29.24 | 67.32 | 4.56 |

Table 6. Comparison of different transition embeddings on the AutoTransition [27] test set in terms of R@k (%) and mean rank. All the rows use the same recommendation model training pipeline from [27] and the only difference is the pre-computed fixed embedding for the transitions.

only spatial-temporal encoder and in-batch InfoNCE loss achieves an average R@1 score of 31.2%. Adding the embedding queue loss term (‘Baseline + \mathcal{L}_q ’) brings 5.4% improvement on the R@1 accuracy, indicating the effectiveness of the \mathcal{L}_q in Eq. 2. The R@1 is further improved by 3.4% when adding guidance tokens in the spatial encoder (‘Baseline + \mathcal{L}_q + GT’). Instead, deploying the guided embedding decoder (‘Baseline + \mathcal{L}_q + GD’) also gains 12.4% improvement on R@1 over ‘Baseline + \mathcal{L}_q ’. The performance is further improved when all the modules are employed (‘Baseline + \mathcal{L}_q + GT + GD’), demonstrating the effectiveness of the guidance architecture.

Embedding Centers. Tab. 5 shows the ablation study using different embedding centers as guidance tokens. Both ‘Default 6 Types’ and ‘K-Means’ perform well with a significant performance boost over ‘None’ (no embedding centers), indicating our guidance architecture is generic for different clustering methods. The default version with 6 editing component types performs slightly better on Edit3K, but the k-means clustering centers are more flexible for other

tasks.

5.5. Transition Recommendation

We conduct experiments on transition recommendation as a downstream task to validate the generalization ability of our learned universal representation. In [27], the embeddings of transitions are pre-computed with a classification model trained on AutoTransition dataset, and the embeddings are fixed during the training of the recommendation model. As shown in Fig. 7, we follow [27] to train transition recommendation models which take a raw video as input and generate ranking scores for a set of transitions. We replace the pre-computed transition embeddings with other alternative methods to validate the benefit of a strong representation on downstream tasks. We follow [27] to report R@k and mean rank for evaluation.

Tab. 6 shows that the embedding of the proposed method trained on AutoTransition datasets (‘Ours-A’) outperforms the state-of-the-art result in [27] (‘Classification’), indicating the superiority of the proposed architecture. Since

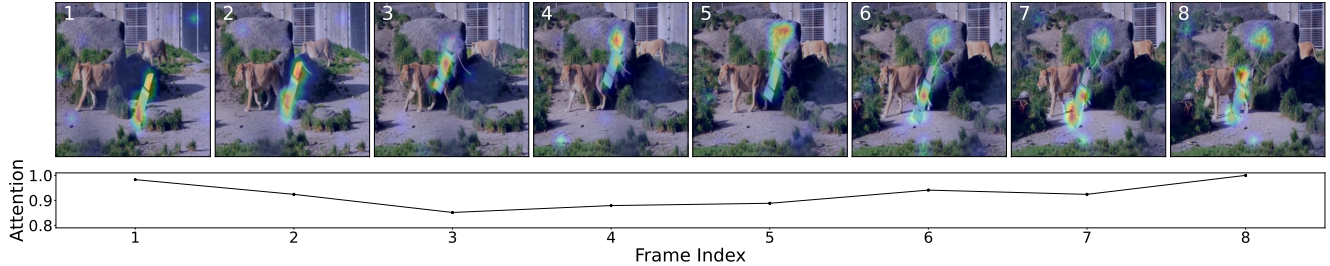


Figure 8. Visualization of the attention map in the spatial and temporal encoder. The first row shows the spatial attention maps overlaid on the 8 input frames, the bottom axis shows the temporal attention value for each frame. The model focuses on the lipstick-shaped sticker for all the frames without explicit spatial supervision. Best viewed on the screen with zoom-in.

the transitions in AutoTransition dataset are included in our Edit3K dataset, we further adopt the pre-computed embedding on Edit3K (‘Ours-E’) and it brings additional performance boosts, indicating the superiority of our diverse and balanced dataset. *Note that all the rows use the same recommendation method and the only difference is the pre-computed transition embeddings, a slight performance boost could indicate significant improvement on representation learning.*

5.6. Attention Visualization

Fig. 8 shows both the spatial and temporal attention map of our model by visualizing the multi-head self-attention/cross-attention module of the last transformer layer in the spatial encoder and temporal encoder, respectively. The output of our model highly depends on the highlighted regions. In Fig. 8, a lipstick-shape sticker is added in the middle of the scene with moving animals. Although our model is not trained with explicit segmentation supervision, our model learns to focus on the sticker and ignore the background changes when both the sticker and the background scene are moving. The temporal attention values of the eight frames are similar to each other, as the sticker appears on all the frames. More results can be seen in the **supplementary material**.

6. Conclusion

We introduce the first large-scale editing components dataset with 618,800 rendered videos covering 6 major types of editing components, which can benefit related downstream tasks. We further propose a novel embedding guidance architecture and a specifically designed contrastive loss for editing component representation learning. It achieves state-of-the-art performance on both editing components retrieval and a major downstream task, *i.e.* transition recommendation. The user study also demonstrates that the learned embedding distribution of our model is better than that of existing methods.

One limitation is that our current model uses low frames

per second (FPS), which cannot handle extremely fast motion or appearance change. In addition, some editing components may have very small changes on the raw videos which is very challenging for our model to recognize without raw video as input. How to efficiently take advantage of the raw videos is worth exploring in the future.

With the rapid growth of video-sharing platforms, edited videos have become one of the major data sources on the Internet. This work serves as a solid step toward understanding video editing for better recommendation, security, etc. The authors do not foresee any negative social impact.

References

- [1] <https://www.capcut.com/>. **3**
- [2] Anurag Arnab, Mostafa Dehghani, Georg Heigold, Chen Sun, Mario Lučić, and Cordelia Schmid. Vivit: A video vision transformer. In *Proceedings of the IEEE/CVF international conference on computer vision*, pages 6836–6846, 2021. **2**
- [3] Nicolas Carion, Francisco Massa, Gabriel Synnaeve, Nicolas Usunier, Alexander Kirillov, and Sergey Zagoruyko. End-to-end object detection with transformers. In *European conference on computer vision*, pages 213–229. Springer, 2020. **5**
- [4] Duygu Ceylan, Chun-Hao P Huang, and Niloy J Mitra. Pix2video: Video editing using image diffusion. In *Proceedings of the IEEE/CVF International Conference on Computer Vision*, pages 23206–23217, 2023. **2**
- [5] Xinlei Chen and Kaiming He. Exploring simple siamese representation learning. In *Proceedings of the IEEE/CVF conference on computer vision and pattern recognition*, pages 15750–15758, 2021. **2**
- [6] Jia Deng, Wei Dong, Richard Socher, Li-Jia Li, Kai Li, and Li Fei-Fei. Imagenet: A large-scale hierarchical image database. In *2009 IEEE conference on computer vision and pattern recognition*, pages 248–255. Ieee, 2009. **3**
- [7] Jacob Devlin, Ming-Wei Chang, Kenton Lee, and Kristina Toutanova. Bert: Pre-training of deep bidirectional transformers for language understanding. *arXiv preprint arXiv:1810.04805*, 2018. **5**
- [8] Alexey Dosovitskiy, Lucas Beyer, Alexander Kolesnikov, Dirk Weissenborn, Xiaohua Zhai, Thomas Unterthiner,

- Mostafa Dehghani, Matthias Minderer, Georg Heigold, Sylvain Gelly, et al. An image is worth 16x16 words: Transformers for image recognition at scale. In *International Conference on Learning Representations*, 2020. 4
- [9] Christoph Feichtenhofer, Haoqi Fan, Jitendra Malik, and Kaiming He. Slowfast networks for video recognition. In *Proceedings of the IEEE/CVF international conference on computer vision*, pages 6202–6211, 2019. 1, 2
- [10] Christoph Feichtenhofer, Haoqi Fan, Bo Xiong, Ross Girshick, and Kaiming He. A large-scale study on unsupervised spatiotemporal representation learning. In *Proceedings of the IEEE/CVF Conference on Computer Vision and Pattern Recognition*, pages 3299–3309, 2021. 2
- [11] Nathan Frey, Peggy Chi, Weilong Yang, and Irfan Essa. Automatic non-linear video editing transfer. *arXiv preprint arXiv:2105.06988*, 2021. 2
- [12] Ian Goodfellow, Jean Pouget-Abadie, Mehdi Mirza, Bing Xu, David Warde-Farley, Sherjil Ozair, Aaron Courville, and Yoshua Bengio. Generative adversarial networks. *Communications of the ACM*, 63(11):139–144, 2020. 2
- [13] Kaiming He, Haoqi Fan, Yuxin Wu, Saining Xie, and Ross Girshick. Momentum contrast for unsupervised visual representation learning. In *Proceedings of the IEEE/CVF conference on computer vision and pattern recognition*, pages 9729–9738, 2020. 2, 4, 5, 6
- [14] Kaiming He, Xinlei Chen, Saining Xie, Yanghao Li, Piotr Dollár, and Ross Girshick. Masked autoencoders are scalable vision learners. In *Proceedings of the IEEE/CVF conference on computer vision and pattern recognition*, pages 16000–16009, 2022. 1, 2, 6
- [15] Jonathan Ho, Ajay Jain, and Pieter Abbeel. Denoising diffusion probabilistic models. *Advances in neural information processing systems*, 33:6840–6851, 2020. 2
- [16] Will Kay, Joao Carreira, Karen Simonyan, Brian Zhang, Chloe Hillier, Sudheendra Vijayanarasimhan, Fabio Viola, Tim Green, Trevor Back, Paul Natsev, et al. The kinetics human action video dataset. *arXiv preprint arXiv:1705.06950*, 2017. 2
- [17] Diederik P Kingma and Jimmy Ba. Adam: A method for stochastic optimization. *arXiv preprint arXiv:1412.6980*, 2014. 5
- [18] Sharath Koorathota, Patrick Adelman, Kelly Cotton, and Paul Sajda. Editing like humans: a contextual, multimodal framework for automated video editing. In *Proceedings of the IEEE/CVF Conference on Computer Vision and Pattern Recognition*, pages 1701–1709, 2021. 2
- [19] Jun Hao Liew, Hanshu Yan, Jianfeng Zhang, Zhongcong Xu, and Jiashi Feng. Magicedit: High-fidelity and temporally coherent video editing. *arXiv preprint arXiv:2308.14749*, 2023. 2
- [20] Ilya Loshchilov and Frank Hutter. Sgdr: Stochastic gradient descent with warm restarts. In *International Conference on Learning Representations*, 2016. 5
- [21] Aaron van den Oord, Yazhe Li, and Oriol Vinyals. Representation learning with contrastive predictive coding. *arXiv preprint arXiv:1807.03748*, 2018. 2, 4, 5
- [22] Tian Pan, Yibing Song, Tianyu Yang, Wenhao Jiang, and Wei Liu. Videomoco: Contrastive video representation learning with temporally adversarial examples. In *Proceedings of the IEEE/CVF conference on computer vision and pattern recognition*, pages 11205–11214, 2021. 2, 6
- [23] Adam Paszke, Sam Gross, Francisco Massa, Adam Lerer, James Bradbury, Gregory Chanan, Trevor Killeen, Zeming Lin, Natalia Gimelshein, Luca Antiga, et al. Pytorch: An imperative style, high-performance deep learning library. *Advances in neural information processing systems*, 32, 2019. 5
- [24] Alec Radford, Jong Wook Kim, Chris Hallacy, Aditya Ramesh, Gabriel Goh, Sandhini Agarwal, Girish Sastry, Amanda Askell, Pamela Mishkin, Jack Clark, et al. Learning transferable visual models from natural language supervision. In *International conference on machine learning*, pages 8748–8763. PMLR, 2021. 5
- [25] Robin Rombach, Andreas Blattmann, Dominik Lorenz, Patrick Esser, and Björn Ommer. High-resolution image synthesis with latent diffusion models. In *Proceedings of the IEEE/CVF conference on computer vision and pattern recognition*, pages 10684–10695, 2022. 2
- [26] Xindi Shang, Tongwei Ren, Jingfan Guo, Hanwang Zhang, and Tat-Seng Chua. Video visual relation detection. In *ACM International Conference on Multimedia*, Mountain View, CA USA, 2017. 3
- [27] Yaojie Shen, Libo Zhang, Kai Xu, and Xiaojie Jin. Autotransition: Learning to recommend video transition effects. In *European Conference on Computer Vision*, pages 285–300. Springer, 2022. 2, 3, 4, 8
- [28] Zhan Tong, Yibing Song, Jue Wang, and Limin Wang. Videomae: Masked autoencoders are data-efficient learners for self-supervised video pre-training. *Advances in neural information processing systems*, 35:10078–10093, 2022. 2, 6
- [29] Du Tran, Heng Wang, Lorenzo Torresani, and Matt Feiszli. Video classification with channel-separated convolutional networks. In *Proceedings of the IEEE/CVF international conference on computer vision*, pages 5552–5561, 2019. 2
- [30] Laurens Van der Maaten and Geoffrey Hinton. Visualizing data using t-sne. *Journal of machine learning research*, 9(11), 2008. 7
- [31] Ashish Vaswani, Noam Shazeer, Niki Parmar, Jakob Uszkoreit, Llion Jones, Aidan N Gomez, Łukasz Kaiser, and Illia Polosukhin. Attention is all you need. *Advances in neural information processing systems*, 30, 2017. 4, 5
- [32] Limin Wang, Bingkun Huang, Zhiyu Zhao, Zhan Tong, Yinan He, Yi Wang, Yali Wang, and Yu Qiao. Videomae v2: Scaling video masked autoencoders with dual masking. In *Proceedings of the IEEE/CVF Conference on Computer Vision and Pattern Recognition*, pages 14549–14560, 2023. 2
- [33] Chen Wei, Haoqi Fan, Saining Xie, Chao-Yuan Wu, Alan Yuille, and Christoph Feichtenhofer. Masked feature prediction for self-supervised visual pre-training. In *Proceedings of the IEEE/CVF Conference on Computer Vision and Pattern Recognition*, pages 14668–14678, 2022. 2

- [34] Chao-Yuan Wu, R Manmatha, Alexander J Smola, and Philipp Krahenbuhl. Sampling matters in deep embedding learning. In *Proceedings of the IEEE international conference on computer vision*, pages 2840–2848, 2017. [5](#)
- [35] Shuai Yang, Yifan Zhou, Ziwei Liu, and Chen Change Loy. Rerender a video: Zero-shot text-guided video-to-video translation. *arXiv preprint arXiv:2306.07954*, 2023. [2](#)
- [36] He Zhang, Jianming Zhang, Federico Perazzi, Zhe Lin, and Vishal M Patel. Deep image compositing. In *Proceedings of the IEEE/CVF winter conference on applications of computer vision*, pages 365–374, 2021. [3](#)